



## Comparative study between a gravity-based and peristaltic pump for intravenous infusion with respect to the generation of proteinaceous microparticles

Shavron Hada<sup>a,1</sup>, Sunkyoung Ji<sup>a,1</sup>, Ye Na Lee<sup>a</sup>, Ki Hyun Kim<sup>a</sup>, Ravi Maharjan<sup>a</sup>, Nam Ah Kim<sup>b,\*</sup>, Jukka Rantanen<sup>c</sup>, Seong Hoon Jeong<sup>a,\*</sup>

<sup>a</sup> BK21 FOUR Team and Integrated Research Institute for Drug Development, College of Pharmacy, Dongguk University, Gyeonggi 10326, Republic of Korea

<sup>b</sup> College of Pharmacy, Mokpo National University, Jeonnam 58554, Republic of Korea

<sup>c</sup> Department of Pharmacy, Faculty of Health and Medical Sciences, University of Copenhagen, Universitetsparken 2, DK-2100 Copenhagen, Denmark

### ARTICLE INFO

#### Keywords:

Infusion pump  
Peristaltic pump  
Gravity infusion  
Protein aggregation  
Subvisible particle  
Flow imaging

### ABSTRACT

Subvisible particles generated during the preparation or administration of biopharmaceuticals might increase the risk of immunogenicity, inflammation, or organ dysfunction. To investigate the impact of an infusion system on the level of subvisible particles, we compared two types of infusion sets based on peristaltic movement (Medifusion DI-2000 pump) and a gravity-based infusion system (Accu-Drip) using intravenous immunoglobulin (IVIG) as a model drug. The peristaltic pump was found to be more susceptible to particle generation compared to the gravity infusion set owing to the stress generated due to constant peristaltic motion. Moreover, the 5- $\mu$ m in-line filter integrated into the tubing of the gravity-based infusion set further contributed to the reduction of particles mostly in the range  $\geq 10 \mu\text{m}$ . Furthermore, the filter was also able to maintain the particle level even after the pre-exposure of samples to silicone oil-lubricated syringes, drop shock, or agitation. Overall, this study suggests the need for the selection of an appropriate infusion set equipped with an in-line filter based on the sensitivity of the product.

### 1. Introduction

Intravenous (IV) infusion is a common route of delivery for biopharmaceuticals, accounting for about 63% of protein therapeutics as of 2018 (Luo et al., 2020). IV infusion therapeutics are prepared by injecting a calculated amount of the drug into an IV infusion bag through syringes, followed by mixing and administration at controlled flow rates (if necessary) through medical tubing. Each of these steps, even when strictly followed based on the product label and guidelines, can potentially expose proteins to various stresses, prompting the generation of particles (Werner and Winter, 2015).

Particulate matter is generally monitored and regulated in the finished drug product (Besheer, 2017; Glover et al., 2013; Kumru et al., 2012). Besides, excipients are being added in formulations to reduce the susceptibility of proteins to the stresses through extensive screening processes (Kamerzell et al., 2011; Messina and Woys, 2022; Panchal

et al., 2022; Svilenov et al., 2023). However, once the therapeutic proteins are released into the market, there is limited control or only a visual inspection of the factors that contribute to their generation and affect their quality and integrity (Nejadnik et al., 2018). Moreover, the magnitude and nature of mechanical stress or surface exposures could differ in actual clinical settings. As per an observational study in a clinical setting, there were several such incidences including agitation of vials, back-and-forth movement of the plastic syringes, and dropping of IV bags (Jiskoot et al., 2017). Such mishandlings could expose protein therapeutics to interfacial stresses, inducing subvisible particles (Carpenter et al., 2009; Ghazvini et al., 2016; Kim et al., 2021; Kim et al., 2020; Linkuvienė et al., 2022; Liu et al., 2011; Nejadnik et al., 2018; Randolph et al., 2015; Thirumangalathu et al., 2009; Ueda et al., 2019). Likewise, IV infusion-specific infusion pumps could be another potential source of particle formation since pump systems have been identified as one of the major sources of protein particle formation (Deiringer et al.,

\* Corresponding authors.

E-mail addresses: [shavron.hada@dgu.ac.kr](mailto:shavron.hada@dgu.ac.kr) (S. Hada), [jisunk97@dongguk.edu](mailto:jisunk97@dongguk.edu) (S. Ji), [scht35@dgu.ac.kr](mailto:scht35@dgu.ac.kr) (Y.N. Lee), [kihyun@dongguk.edu](mailto:kihyun@dongguk.edu) (K.H. Kim), [raavii@dgu.ac.kr](mailto:raavii@dgu.ac.kr) (R. Maharjan), [namahk87@mnu.ac.kr](mailto:namahk87@mnu.ac.kr) (N.A. Kim), [jukka.rantanen@sund.ku.dk](mailto:jukka.rantanen@sund.ku.dk) (J. Rantanen), [shjeong@dongguk.edu](mailto:shjeong@dongguk.edu) (S.H. Jeong).

<sup>1</sup> Authors contributed equally.

<https://doi.org/10.1016/j.ijpharm.2023.123091>

Received 26 January 2023; Received in revised form 12 May 2023; Accepted 25 May 2023

Available online 1 June 2023

0378-5173/© 2023 Elsevier B.V. All rights reserved.

\*최근 동국대학교 연구에서 Accu-Drip/ Accu-Valve가 생물학적 제제 주사시 발생할 수 있는 단백질미립자 생성에서 인퓨전펌프보다 우수하다는 것이 확인이 되어 해외논문 international journal of pharmaceutics (Impact factor: 6.51)에 투고하여 게재가 승인이 되었습니다.

2022; Dreckmann et al., 2020; Gomme et al., 2006; Her and Carpenter, 2020; Her et al., 2020; Wu and Randolph, 2020).

Peristaltic pumps are commonly used in infusion sets as they allow accurate calibration of the flow rate while keeping it constant, making them ideal for precise dosing control (Formato et al., 2019; Pollo et al., 2019). The pump works through a positive displacement of fluid generated by the periodical pressing of a tube segment against the pump housing (Klespitz and Kovács, 2014). Although the infusion peristaltic pumps studied by Deiringer et al. and Wu et al. mainly cover the peristaltic pumps used in the fill and finish procedures, with a similar working mechanism of positive displacement through repeated compression and expansion, the protein particulates in infusion pumps can be produced based on the adsorption of proteins onto the tubing surface followed by disruption during operation and are released as a protein film (Deiringer et al., 2022; Wu and Randolph, 2020). To prevent particles from entering into the patient's systemic circulation, tubing sets are available with in-line filters ranging from 0.2 to 15  $\mu\text{m}$  pore size (Werner and Winter, 2015). However, particles larger than 20  $\mu\text{m}$  have been detected even when 0.2  $\mu\text{m}$  and 1.2  $\mu\text{m}$  in-line filters were used (Pardeshi et al., 2017). Alternatively, a gravity-based infusion set, also known as an IV drip, allows the flow by utilizing the gravitational force which normally consists of a drip chamber and a flow regulator. Meanwhile, compared to the infusion pumps, the flow rate in a conventional gravity-based infusion set is less accurate as it depends on the height of the infusion bag or bottle (Crass and Vance, 1985). Nevertheless, unlike the peristaltic pump, it does not involve repeated tubing compression, which leads to a hypothesis that the level of particle generation would be lower than that of peristaltic pumps.

The existence of particulate matter particularly in the subvisible range (i.e., approximately 1–100  $\mu\text{m}$ ) and lower has been a critical challenge in biopharmaceuticals as it poses a higher risk of being undetected in the clinical setting due to their small size and transparency (Carpenter et al., 2009; Kumru et al., 2012; Langille, 2013). Despite the improvements in subvisible particle analysis technologies such as FI technology or background membrane imaging (Fawaz et al., 2023; Helbig et al., 2020), implementing these techniques in a clinical setting (e.g., in-use stability) is less feasible. Infused subvisible particles carry a risk of developing several complications during IV infusions including immunogenic reactions, inflammation, or even organ dysfunction (Ilium et al., 1982; Niehaus et al., 1984; Pardeshi et al., 2021; Turco and Davis, 1971; Van Boxtel et al., 2022). Reflecting on the severity of possible adverse events secondary to the infusion of subvisible particles into patients, and with an intent to suggest a better infusion system, the current study was designed to compare the level of subvisible particles generated in two different types of infusion sets (Table 1 and Fig. 1); 1) Infusion set 1: the MEDIFUSION DI-2000 pump based on peristaltic movement conjugated with a di(2-ethylhexyl) phthalate (DEHP)-free infusion tube, and 2) Infusion set 2: Accu-Drip, a gravity-based infusion system, conjugated with a polyurethane infusion tube with a 5- $\mu\text{m}$  in-line filter. The Accu-Drip system used for the study is an automatic infusion control device that is designed to adjust the flow rate with the help of a drop sensor attached to the drip chamber, making it superior to conventional IV drip systems in accuracy (Hanvit MD Co.). Moreover, the investigation also included the effect of the in-line filter, the use of plastic syringes with silicone oil (SO syringe), and the application of mechanical stresses such as drop shock and agitation stress. Intravenous

gamma globulin (IVIG)—the model drug for the study—was diluted into a 5% dextrose IV bag in defined concentrations using a silicone oil-lubricated syringe or silicone oil-free syringe.

## 2. Materials and methods

### 2.1. Materials

IVIG (IVIG-SN 10%; lot number: 383A21020 and 383A22001), composed of 100 mg/mL humanized IgG and 18.8 mg/mL glycine at pH 4.8, was purchased from GC Biopharma (Gyeonggi, Korea). A 100 mL IV infusion bag of 5% dextrose (Lot. A9V9B44 and 44X4B44) (packaging material: multi-layered non-PVC films, with polypropylene in the surface of contact with the solution) was purchased from Dai Han Pharm. Co., Ltd. (Seoul, Korea). The tubing sets: IV flow regulator set (SRY-400A) (Tube 1) and Accu-Valve-IV set (Tube 2) were purchased from Sungshim Medical Co., Ltd. (Daegu, Korea) and Hanvit MD Co., Ltd. (Daejeon, Korea), respectively. The Medifusion DI-2000 pump based on a peristaltic mechanism was procured from Daiwha Corp., Ltd. (Incheon, Korea), and the electronic infusion controller for gravity flow infusion systems (Accu-Drip) based on the gravitational force was purchased from Hanvit MD Co., Ltd. (Daejeon, Korea). A 22G needle (Lot. 0711108) and IV catheter (Kovax-CATH 24G) (Lot. 0611065) were purchased from Kovax Corporation (Seoul, Korea). A 10 mL syringe from Henke Sass Wolf (Tuttlingen, Germany) was used as a SO-free syringe, and a 10 mL syringe from Kovax (Seoul, Korea) was used as an SO syringe, utilized for withdrawing the IVIG from the vial and injecting into the IV bag for the preparation.

### 2.2. Sample preparation

Desired amounts of IVIG (for diluted concentrations of 20 mg/mL and 60 mg/mL, based on the dosage recommendation for pediatric patients weighing 4.2–12.5 kg and 10–30 kg, respectively) were injected into the 5% dextrose IV bag and mixed by gently pressing with the fingers. The flow rate of the infusion was set at 40 mL/h, whereas the samples were collected in a sterile 50 mL falcon tube. The samples were then stored in a refrigerator at 4 °C and analyzed within five days. All samples were prepared in triplicate (n = 3).

### 2.3. Stress testing: 1) bag drop, 2) vial agitation, and 3) silicone oil from a syringe

For bag drop stress, IVIG diluted in a 5% dextrose IV bag was dropped once on the floor from a height of about 1 m (n = 3). The stress test was duplicated with the use of either SO syringe or SO-free syringe in introducing IVIG into the IV bags. Agitation stress was performed on a 100 mg/mL IVIG vial, the commercial product itself, using a multimixer set at 40 rpm (Seoulin Bioscience, Gyeonggi, Korea) for five days at 25 °C (n = 3). The agitated IVIG samples were then transferred into the IV bag using either an SO syringe or SO-free syringe, and subsequently infused through the IV tubing related to different infusion sets for sample collection.

**Table 1**

Information on tubing and infusion methods used for the current study.

Infusion method	Flow rate (mL/h)	Tubings	Tubing material	In-line filter	Abbreviation
Peristaltic pump (Medifusion DI-2000)	100	Tube 1 (SRY-400A)	Polyvinyl Chloride, non-DEHP	Absent	Infusion set 1
Gravity dependent (Accu-Drip)	1–350	Tube 2 (Accu-Valve-IV set) Tube 2- <i>rf</i>	Polyurethane (drip chamber: styrene, butadiene copolymer)	Present (5 $\mu\text{m}$ ) Removed	Infusion set 2  Infusion set 2- <i>rf</i>

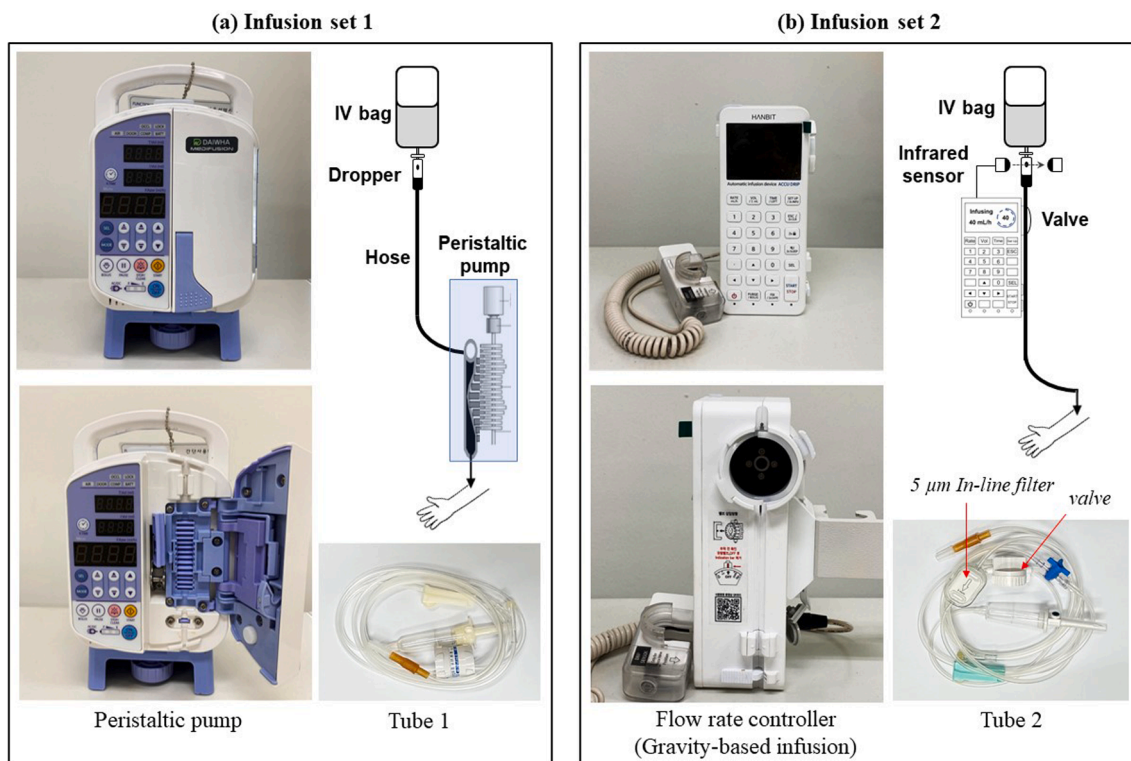


Fig. 1. Images of the infusion sets used in the study as (a) a peristaltic infusion pump with a DEHP-free tubing set (Infusion set 1), and (b) an **Accu-Drip** (gravity-based) infusion system with a polyurethane tubing set (Infusion set 2).

#### 2.4. Size exclusion chromatography (SEC)

SEC analysis was performed in Agilent HPLC 1260 series (CA, USA) with TSKgel® G3000SW<sub>XL</sub> HPLC column (phase diol, 30 cm × 7.8 cm, 5 µm) (Tosoh, Tokyo, Japan) as a stationary phase. The flow rate was set to 0.5 mL/min, with a column temperature of 25 °C. Whereas the samples were eluted using 3 × phosphate-buffered saline (411 mM NaCl, 8.1 mM KCl, 30 mM Na<sub>2</sub>HPO<sub>4</sub>, and 1.8 mM KH<sub>2</sub>PO<sub>4</sub>) adjusted at pH 7.4 as a mobile phase. The injection volume was 20 µL and the UV detector was set at 280 nm. All the samples were diluted to 5 mg/mL before analysis. Monomer contents were calculated using the following equation:

$$\text{Remaining monomer (\%)} = (A_t/A_0) \times 100$$

where  $A_t$  is the area of the monomer of the samples collected after infusion and  $A_0$  is the area of the monomer of 100 mg/mL IVIG with 18.8 mg/mL glycine buffer at pH 4.8 before infusion.

#### 2.5. Light obscuration (LO)

Particle concentrations were analyzed by the HIAC 9703 + liquid particle counter (Beckman Coulter Inc., CA, USA) equipped with a 1-mL syringe pump. Before each analysis, the fluid path was rinsed with deionized water filtered through a 0.2 µm Minisart® NML surfactant-free cellulose acetate syringe filter (Sartorius AG, Goettingen, Germany), followed by particle count measurement to assure cell cleanliness. A value of < 10 particles (p)/mL was considered an acceptable background value. 200 µL of samples were measured each time and an average of the third to fifth scans were used to calculate the mean and standard deviation (the first and last scans were discarded). Each sample and its replicates were measured in triplicate. Particles of sizes  $\geq 2$  µm,  $\geq 5$  µm,  $\geq 10$  µm, and  $\geq 25$  µm were acquired through the PhamSpec software (version 3.5.32) provided with the instrument. The data were then arranged within the size ranges of 2–10 µm, 10–25 µm, and greater

than 25 µm.

#### 2.6. Flow imaging microscopy (FI)

Particle concentrations along with their morphologies were analyzed using a FlowCam 8100 series equipped with a FOV80 flow cell (80 µm depth × 700 µm width) and a 10-fold magnification camera (Fluid Imaging Technologies Inc., ME, USA). Before the analysis, calibration was performed with 15 µm polystyrene beads. Before running each sample, measurements were performed for 0.2-µm filtered deionized water to assure fluid path and cell cleanliness (a particle concentration < 50 p/mL was deemed as an acceptable background value). One milliliter of the sample was loaded, and 0.2 mL each was measured 5 times with a flow rate set at 0.1 mL/min. The auto image rate was set at 10 frames per second leading to a theoretical efficiency of 39.3 percent. The particle concentration (p/mL) is calculated using the Visual spreadsheet software (version 4.17.14) by dividing the particle count by the fluid volume imaged (mL) defined after analysis. An analysis of the third to fifth scans was averaged for the calculation of mean values based on area-based diameter (ABD). Data analyses were performed using the.

#### 2.7. Attenuated total reflectance FT-IR spectroscopy

The Nicolet iS5 spectrophotometer (Thermo Fisher Scientific, Waltham, MA, USA) with an iD5 diamond attenuated total reflectance was utilized to identify the plasticizer composition of the infusion tubes. For identification of the plasticizers, a portion of the tubing was cut through both ends (15 cm) while 5 mL hexane was pipetted into the tube and collected into a beaker. The hexane was then evaporated by heating the beaker at 80 °C until the weight of the beaker remained constant. The dried residue was re-dissolved in 100 µL of hexane prior to analysis. 5 µL of the prepared samples were then placed on the crystal plate and dried for 5 min. 64 interferograms were recorded within the range of 4000  $\text{cm}^{-1}$  to 400  $\text{cm}^{-1}$  in a single beam mode with a resolution of 4  $\text{cm}^{-1}$ .

Nicolet Omnic software version 8.2.387 was then used to analyze the sample spectra.

## 2.8. Viscosity

Viscosity was measured using an m-VROC viscometer with a 18RC05100200 sensor (Rheosense Inc., CA, USA). Water was circulated continuously using a Digital Precise Circulation Water Bath (Daihan Scientific, Seoul, Korea) keeping the temperature constant at 25 °C. All samples were measured after confirming the viscosity of deionized water as 1.0–1.1 mPa·s with an  $R^2$  value of  $\geq 0.98$  under the shear rate of  $6000 \text{ s}^{-1}$ . The sample was then prepared by diluting IVIG in 18.8 mg/mL glycine buffer at concentrations ranging from 60 mg/mL to 100 mg/mL. Each sample was loaded into a 500- $\mu\text{L}$  Hamilton syringe while the measurement was performed by increasing the shear rate gradually in seven steps from  $2100 \text{ s}^{-1}$  to  $9900 \text{ s}^{-1}$ .

## 2.9. Statistical analysis

The student's *t*-test was used to compare the results from FI and LO in Microsoft Excel. Statistical significance for each analysis was denoted by a 1-tailed *p*-value divided into three categories as:  $< 0.05$  (\*),  $< 0.01$

(\*\*), and  $< 0.001$  (\*\*\*). All the data are presented as mean values and standard deviations.

Principal component analysis (PCA) was employed to identify the contribution of particle characteristics in defining the proteinaceous subvisible particles generated through various stresses. The particle characteristic parameters obtained through FI were narrowed down through PCA using JMP Pro® version 16.2.0 (SAS Institute Inc., Cary, NC, USA). The classification was predicted on the basis of positive or negative sign of each principal component composed of identified parameters.

## 3. Results and discussion

### 3.1. Comparison of infusion sets: Particle concentration during administration

Fig. 2a and 2b exhibit the subvisible particle concentration of IVIG in 5% dextrose before and after infusion sets by LO and FI, respectively. The particle concentrations analyzed by LO before infusion were detected (i.e., remarked as 'IVIG (diluted)') as 47 p/mL, 0 p/mL, and 0 p/mL at 20 mg/mL, which increased to 100 p/mL, 10 p/mL, and 3 p/mL at 60 mg/mL in the size range of 2–10  $\mu\text{m}$ , 10–25  $\mu\text{m}$ , and  $\geq 25 \mu\text{m}$ ,

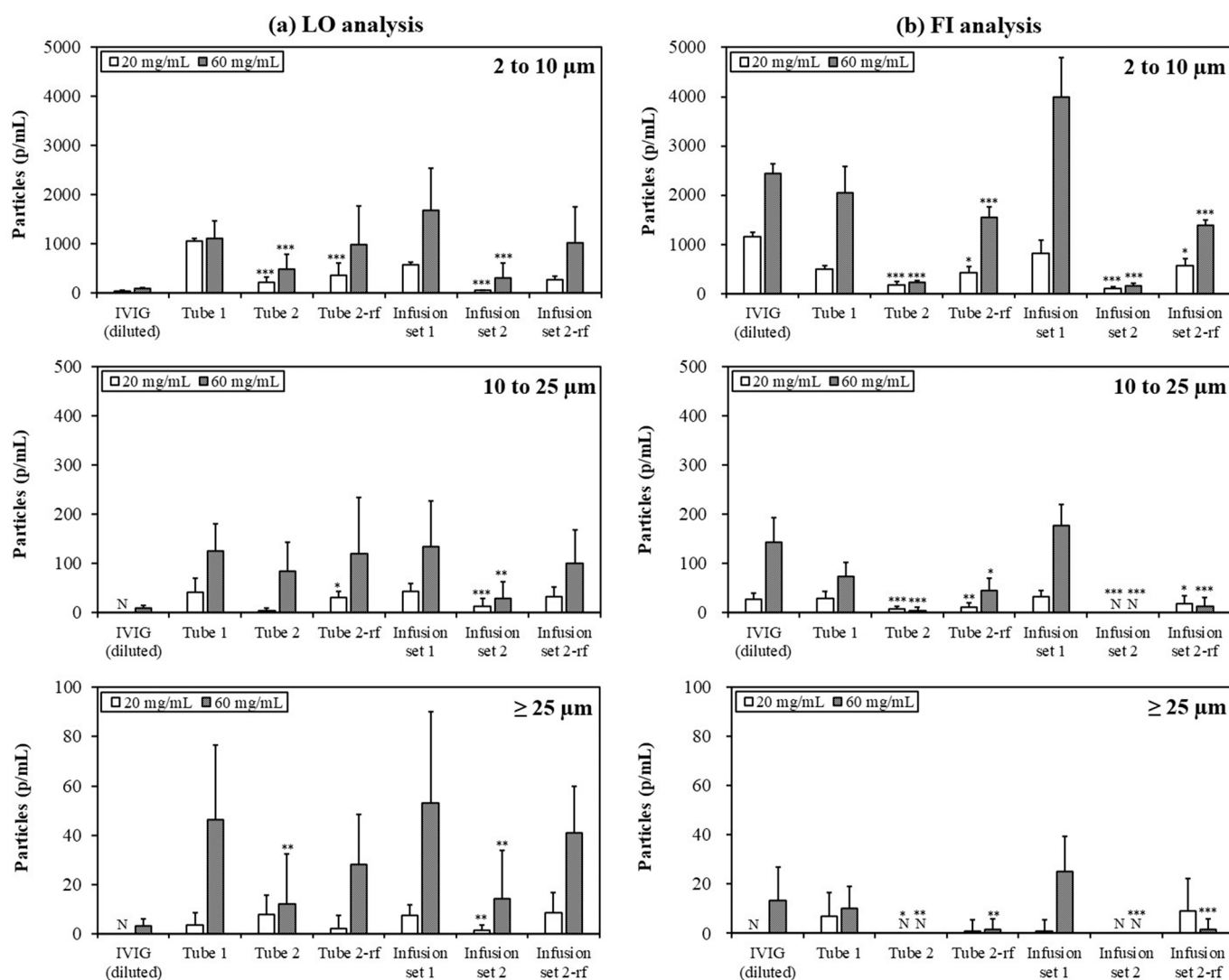


Fig. 2. Bar graph of subvisible particles released through the different tubing and infusion sets analyzed by (a) LO and (b) FI. \* $p < 0.05$ , \*\* $p < 0.01$ , and \*\*\* $p < 0.001$  indicate statistical significance of particle concentration as Tube 1 vs. Tube 2 and Tube 2-rf, and Infusion set 1 vs. Infusion set 2 and Infusion set 2-rf ( $n = 9$ ). (N: no particles detected).

respectively, suggesting an increase in particle counts and size at a higher IVIG concentration (Fig. 2a). However, the numbers were found to be within the limits stated in the USP chapter <787> ( $< 25$  p/mL for  $\geq 10$   $\mu\text{m}$ , and  $< 3$  p/mL for  $\geq 25$   $\mu\text{m}$ ). Conversely, a notable increase in the particle concentration overpassed the limit when the same samples were analyzed by FI, specifically within the range of 2–25  $\mu\text{m}$  (more than 10 times compared to LO) (Fig. 2b). The particle counts and its sizes were found to be higher at higher IVIG concentrations. Initially, the repackaged IVIG was analyzed after passing through both Tubes 1 and 2 (i.e., infusion tubing) to compare the effects of different tubing sets in the particle formation. The sample passed through Tube 2 exhibited a relatively lower number of particles in all size ranges compared to Tube 1 in both LO and FI. Based on FI, the particle counts were reduced to around 3 and 8 times at the range 2–10  $\mu\text{m}$ , and around 4 and 18 times at the range 10–25  $\mu\text{m}$  at the concentrations 20 mg/mL and 60 mg/mL, respectively. The limited number of particles greater than 10  $\mu\text{m}$  in Tube 2 could be due to the adsorption of proteins onto the liquid–solid interfaces of the downstream side of the membrane, filter housing, and wall of the tubing, which eventually sloughs off and forms proteinaceous particles as demonstrated by Pardeshi et al. (Pardeshi et al., 2017). Besides, no particles were detected in Tube 2 with a size  $\geq 25$   $\mu\text{m}$  (Fig. 2b). The prominent reduction can be attributed mainly to the presence of a 5- $\mu\text{m}$  in-line filter in Tube 2 (Allcutt et al., 1983; Werner and Winter, 2015). Moreover, the particle level increased in all size ranges once the integrated filter was detached (Tube 2-rf; Fig. 2b). The particle concentrations in samples passed through Tube 1 and Tube 2 remained lower than the samples prior to infusion, which could be due to the adsorption of the proteins on the hydrophobic inner wall of the tubing surface owing to its amphiphilic nature (Sherwin et al., 2014; Tzannis et al., 1997; Zahid et al., 2008). On the other hand, LO is dependent on particle capacity to block light, particles with a near refractive index to that of the solution tend to be undersized or undercounted (Yoneda et al., 2019). Moreover, low reproducibility and higher standard deviation were observed in the LO data as displayed in Fig. 2a. Hence, the particles were solely discussed using FI for further studies.

To evaluate the impact of different infusion sets on the particulate concentration, two infusion sets were tested; a peristaltic pump used in conjunction with Tube 1 (Infusion set 1) and an Accu-Drip used in conjunction with Tube 2 (Infusion set 2). Both LO and FI exhibited an increase in the particle count in Infusion set 1, which was specifically evident through FI analysis with about 1.5-fold and 2-fold particles compared to Tube 1 alone (Fig. 2b). Conversely, the particles remained relatively constant with the use of Infusion set 2. This result could be due to: 1) the different infusion mechanisms, and/or 2) the presence of the in-line filter. To confirm this and to observe the effect of the Accu-drip infusion system alone, the in-line filter was removed (remarked as 'Infusion set 2-rf'). The particle counts subsequently increased at both IVIG concentrations, indicating the number of particles filtered. However, it should be noted that the particle count was yet lower (i.e., 56 p/mL, 18 p/mL, and 9 p/mL at 20 mg/mL, and 1380 p/mL, 13 p/mL, and 1 p/mL at 60 mg/mL in 2–10  $\mu\text{m}$ , 10–25  $\mu\text{m}$ , and  $\geq 25$   $\mu\text{m}$ , respectively) compared to Infusion set 1 (822 p/mL, 33 p/mL, and 1 p/mL at 20 mg/mL, and 3991 p/mL, 177 p/mL, and 25 p/mL at 60 mg/mL in 2–10  $\mu\text{m}$ , 10–25  $\mu\text{m}$ , and  $\geq 25$   $\mu\text{m}$ , respectively). The comparison indicates the different infusion set stresses in the particle concentration. Shear stresses are generally known to cause protein denaturation and aggregation when they are transferred using pumps (Cromwell et al., 2006; Dreckmann et al., 2020; Maa and Hsu, 1996; Thomas and Geer, 2011). However, linear peristaltic pumps are known to cause the least amount of shear stress compared to the radial peristaltic pump (Dreckmann et al., 2020). Nevertheless, a study by Deiringer et al. confirmed that interfacial adsorption could play a major role in the generation of proteinaceous microparticles in peristaltic pumps (Deiringer and Friess, 2022a). Moreover, as previously mentioned, continuous squeezing of the infusion tubing by the actuators could trigger the disruption of the protein film, releasing the adsorbed protein layers into the bulk of the

solution in the form of microparticles (Deiringer et al., 2022; Pardeshi et al., 2017; Wu and Randolph, 2020). Supplementarily, the model drug IVIG used for this study is void of the surfactants included in biopharmaceutical formulations to prevent interfacial adsorption (Deiringer and Friess, 2022a; Khan et al., 2015; Kim et al., 2014), which made the product more vulnerable to interfacial adsorption onto the inner surface of the tubing material. Hence, it can be stated that both the infusion mechanism and the existence of an in-line filter improved the performance of Infusion set 2 in terms of minimizing the generation and transit of subvisible particles through the line.

### 3.2. Nature of tubing material and particle formation

Aside from the pump mechanism, tubing materials also have a significant impact on particle production. (Deiringer and Friess, 2022b). Tubings made of polyvinyl chloride (PVC) (as in Tube 1) are quite commonly used for infusion, owing to their durability, chemical resistance, and low cost (Al Salloum et al., 2017; Bernard et al., 2015). However, due to their low flexibility, plasticizers may be added at concentrations as high as 30–40% (w/w) (Rock et al., 1986) which often leaches into the infused solution.

To determine the presence or absence of leachable through the tubing materials, 5% dextrose (without drug) was allowed to run through the infusion sets, and collected samples were subsequently tested by FI. As shown in Fig. 3, Infusion set 2 demonstrated the least number of particles, which increased to 4-fold once the filter was removed (size  $\leq 5$   $\mu\text{m}$ ). Whereas Infusion set 1 showed an 8-fold increase in particles with a size greater than 5  $\mu\text{m}$ . Furthermore, the representative FI images demonstrated a prominent presence of spherical-shaped particles with a mean circularity index of greater than 0.8, suggesting the displacement of hydrophobic liquid compound(s) from the tubing material. Hence, to identify the components of the leached compound from the tubing material, hexane was used as a solvent to dissolve the compound, followed by the analysis of dried residues by FT-IR. Interestingly, the FI-IR spectra of residues from Tube 1 (Fig. 4) depicted distinct absorption bands of (di-(2-ethylhexyl) terephthalate) DEHT at 2958, 2928, 2859  $\text{cm}^{-1}$  (methyl C–H stretching), 1719  $\text{cm}^{-1}$  (C=O stretching of O=C–O), 1577  $\text{cm}^{-1}$  (C=C alkene of benzene ring), 1408  $\text{cm}^{-1}$ , 1380  $\text{cm}^{-1}$  ( $\text{CH}_3$  umbrella deformation bend), 1264–1019  $\text{cm}^{-1}$  (C–O ether stretching), and 728  $\text{cm}^{-1}$  (C–H aromatic out-of-plane bend) (Marx, 2019; Matos et al., 2019). Since the use of DEHP has been restricted by European Directive 2007/47/CE (Council, 2007) due to concerns about its toxicological effect in medical devices, alternative plasticizers such as DEHT, trioctyl trimellitate, or di-isononyl-1,2-cyclohexane-dicarboxylate are being used by the manufacturers (Bernard et al., 2015). Moreover, plasticizers such as DEHT are not covalently bound to the PVC surface and are known to migrate from PVC (although much less than DEHP) into the infused solution (Earla and Braslau, 2014; Snell et al., 2020). Furthermore, this migration creates an oil-water interface for protein adsorption leading to the generation of subvisible particles. In addition, the continuous peristaltic motion of the pump into the tubing further eases the release of these plasticizers into the drug solution, as evident in Fig. 3c. Hence, this leads to the conclusion that, the conjugative effect of the tubing material along with the continuous compressive action within the peristaltic pump leading to the release of plasticizer and adsorption and desorption of protein layers in Infusion set 1 led to the higher number of particles.

On the other hand, the FT-IR spectra of Tube 2 did not exhibit distinct plasticizer peaks, indicating a low level of leachable (Fig. 4b). Besides, PU itself is known to have higher tensile strengths, tear resistance, chemical resistance, and abrasion resistance (Szycher), preventing intrinsic sources of particles from the tubing into the drug solution. As a caveat, leachable can also consist of soluble compounds in nano-size, such as additives that can migrate to the PU surface and then be leached in a soluble or solid form. However, only subvisible particles ( $\geq 1$   $\mu\text{m}$ ) are mainly considered in this study. This along with an in-line

**(a) Infusion set 1:  $1563 \pm 75$  p/mL ( $\leq 10 \mu\text{m}$ )****(b) Infusion set 2:  $197 \pm 8$  p/mL ( $\leq 5 \mu\text{m}$ )****(c) Infusion set 2-rf:  $799 \pm 36$  p/mL ( $\leq 5 \mu\text{m}$ )**

**Fig. 3.** Representative FI images of subvisible particles generated by infusion of 5% dextrose solution through (a) Infusion set 1, (b) Infusion set 2, and (c) Infusion set 2-rf.

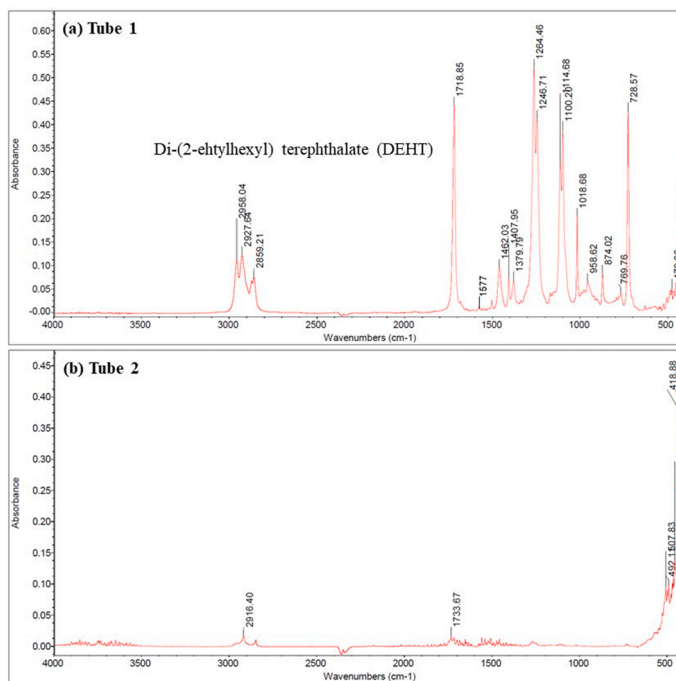


**Fig. 4.** FT-IR spectra of extracted residues from (a) Tube 1 and (b) Tube 2.

filter further reduced the existing subvisible particles in Infusion set 2. Moreover, **Accu-Drip** is solely based on the gravitational force and does not require any mechanical action for passing the liquid, preventing the generation of particles itself in the first place.

### 3.3. Monomeric content and nano-size distribution

SEC was used to compare the monomeric content and soluble

aggregates in the IVIG solution after passing it through two infusion sets (Fig. 5). Although the particle level was relatively higher at 60 mg/mL, its change in monomeric content was less than about 1% compared to Infusion set 2. Current pharmaceutical regulations mandate that IV drug preparations be within 10 % of the nominal concentration consistently during administration (Hung, 2004). Whereas, a 12% difference (1 out of 3 replicates) was observed at 20 mg/mL, when passed through Infusion set 1, exhibiting relatively higher sensitivity of low protein

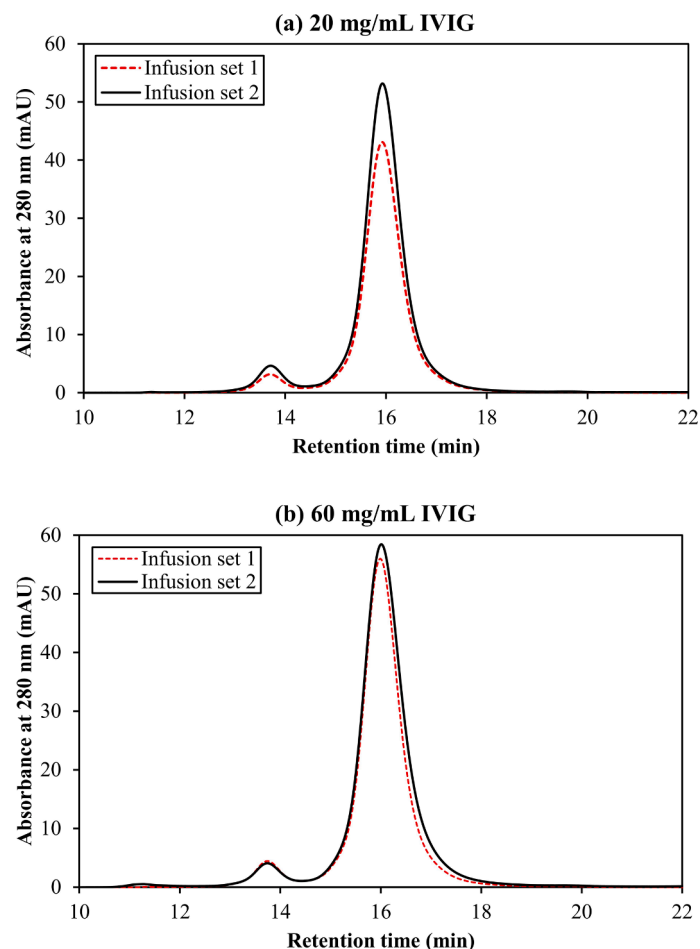


Fig. 5. SEC chromatograms of Infusion sets 1 and 2 at IVIG concentrations of (a) 20 mg/mL and (b) 60 mg/mL.

concentration towards monomer loss. The extensive use of a variety of polymers in IV infusion containers and tubings raises the risk of protein loss through adsorption or subvisible particle formation, particularly at low doses. Moreover, cases of loss in monomer due to adsorption were evident previously in the undiluted protein infusion preparations (Tzannis et al., 1997; Zahid et al., 2008). In the case of peristaltic pumps, the continuous expansion and relaxation of the tubing provoke the constant adsorption, desorption, and film renewal leading to the formation of subvisible particles (Deiringer and Friess, 2023), ultimately causing a loss in the monomer.

Despite the incidence of the decrement in monomer, soluble aggregates remained lower than or equal to Infusion set 2, suggesting less effect on the formation of the soluble aggregates (i.e., < 100 nm). Overall, the SEC results suggest that protein therapeutics at lower concentrations may become more susceptible to monomer loss, which might reduce the effectiveness of the treatment with the use of peristaltic pumps. Consequently, protein loss owing to adsorption onto packaging materials, filters, and tubing, or formation of subvisible particles must be explored and addressed concurrently with formulation development or selection of appropriate administration device, specifically for low-dose products.

### 3.4. Comparison of infusion sets: Stressing IVIG by dropping and agitation

Mishandling protein therapeutics during preparation and administration such as dropping the IV bags, vials, or syringes containing drug products, or vigorous shaking when mixing is more common than we know in clinical settings (Jiskoot et al., 2017). Moreover, the contents are typically administered without additional analysis/inspection if the containers are intact. The unintentional dropping of the containers can

lead to particle formation and aggregation (Randolph et al., 2015). To observe the effects of several mishandlings during the preparation of the IV infusion bag in the particle load along with the additional effect of infusion methods and capacity of the in-line filter, the bag drop and agitation tests were performed as mentioned in section 2.3.

Fig. 6a exhibits the concentration of particles after infusion of stressed 60 mg/mL IVIG through the drop shock and agitation. As expected, the particle levels were elevated in samples before infusion as well as in the samples infused through Infusion set 2. Dropping is known to produce cavitation in liquid pharmaceuticals; even a 10-inch drop onto hard surfaces has been found to produce bubbles (Randolph et al., 2015). In turn, the rapid collapse of bubbles could be followed by free radical formation, a temperature rise, and secondary shock waves resulting in localized protein oxidative and conformational changes (Randolph et al., 2015). Subsequent exposure to the pumping pressure in Infusion set 1 would expectedly further aggravate into a bigger particle (i.e., decreasing particle concentration). Consequently, all the samples passed through Infusion set 1 exhibited reduced particle levels after the drop shock (Fig. 6a). This could be because of the adsorption of proteins into the wall of the tubing and containers or simply particle loss during analysis due to the rapid sedimentation of bigger particles. In a previously observed incidence, a clinically significant reduction in the amount of factor VIII was detected even without any stresses with the loss of activity due to the protein adsorption onto the plastic surface (McLeod et al., 2000). Moreover, a study done with glass vials demonstrated that drop shock additionally substantiates the adsorption of proteins onto the surface which further increased with the drop height (Randolph et al., 2015). Nevertheless, even after the drop shock, IVIG infused through Tube 2, or Infusion set 2 still exhibited a less amount of

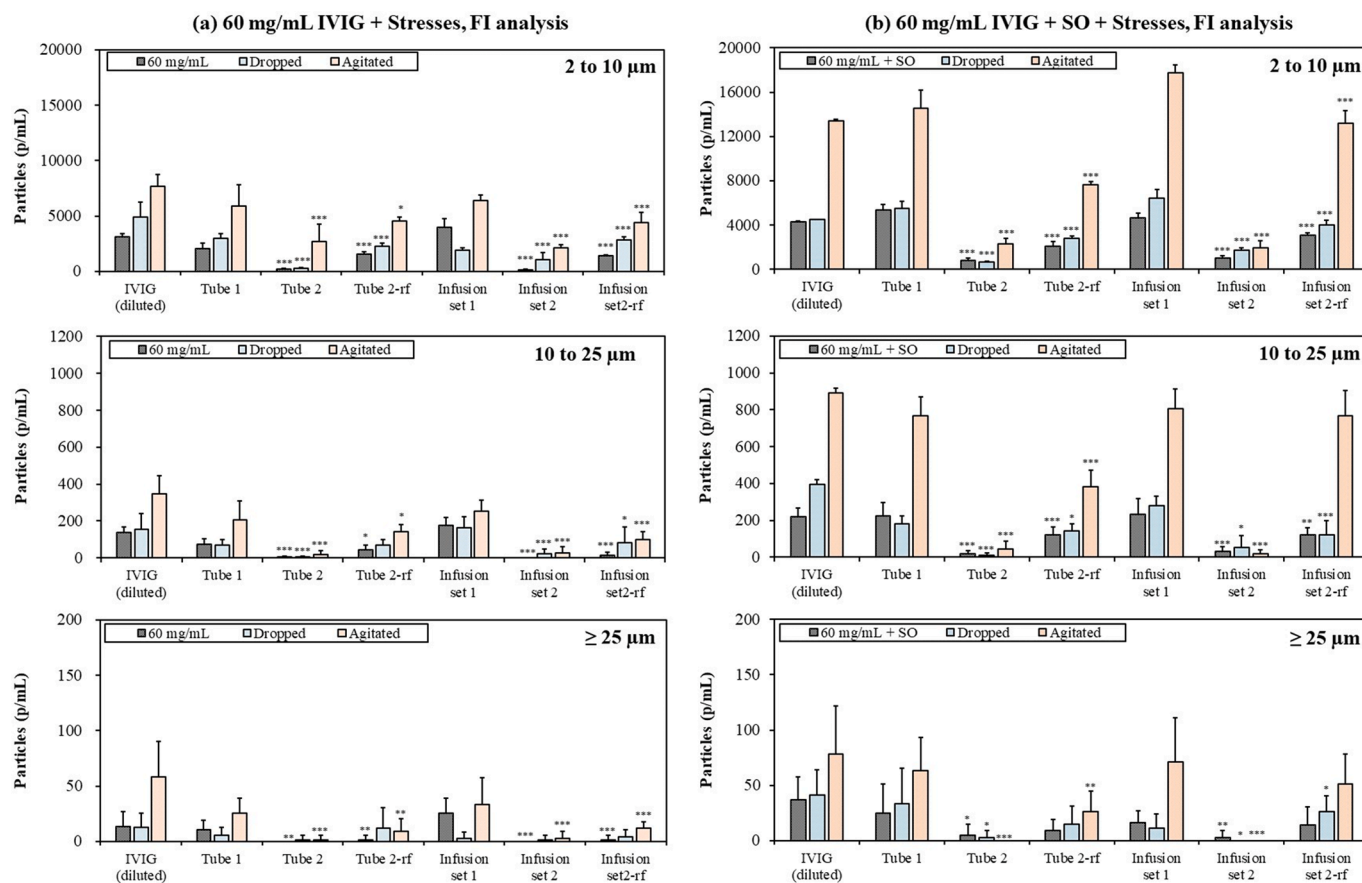


**Fig. 6.** Bar graph of subvisible particles generated after infusion of samples pre-exposed to the drop shock and agitation prepared using (a) an SO syringe or (b) an SO-free syringe. \* $p < 0.05$ , \*\* $p < 0.01$ , and \*\*\* $p < 0.001$  indicate statistical significance of particle concentration as Tube 1 vs. Tube 2 and Tube 2-rf, and Infusion set 1 vs. Infusion set 2 and Infusion set 2-rf ( $n = 9$ ).

subvisible particles in all size ranges compared to Tube 1 alone or Infusion set 1. The particle concentration was 1938 p/mL, 162 p/mL, and 25 p/mL in Infusion set 1, which decreased to 1087 p/mL, 22 p/mL, and 1 p/mL in Infusion set 2 within sizes 2–10  $\mu\text{m}$ , 10–25  $\mu\text{m}$ , and  $\geq 25 \mu\text{m}$ , respectively. The reduction in particles in Infusion set 2 or Tube 2 can again be justified by the inclusion of an in-line filter in Tube 2.

Apart from drop shock, the agitation of vials during the transportation is another example of inevitable mechanical stress that could affect the quality of therapeutic proteins. Consequently, a stress study was performed by agitating the vials containing 100 mg/mL IVIG at 25  $^{\circ}\text{C}$  for five days; the particle level increased throughout the size ranges in all the samples after agitation (Fig. 6a). The adsorption of proteins onto the air–water interface acts as a nucleation site initiating the protein film formation, which is released into the solution leading to the formation of subvisible particles (Ghazvini et al., 2016; Sreedhara et al., 2012). Regardless, the particles were much lower in the sample involving Tube 2 alone or Infusion set 2. Similarly, in the drop test, the reduction was especially evident at the size range  $\geq 10 \mu\text{m}$ , owing to the 5- $\mu\text{m}$  size of the in-line filter. The particle concentration was limited to 19–28 p/mL at the size 10–25  $\mu\text{m}$  and 1–3 p/mL at a size greater than 25  $\mu\text{m}$  with the use of Tube 2 alone or as its infusion sets. As previously observed (Fig. 2b), even without the filter, the particle concentration remained lower than those of the samples infused through Tube 1 alone or its infusion set, suggesting the safety of the gravity-based pump in minimizing the level of subvisible particles.

### 3.5. Comparison of infusion sets: Use of silicone oil (SO) syringes

The elevated particle level of infused 60 mg/mL IVIG prepared using SO syringes is shown in Fig. 6b. In plastic syringes, silicone oil is coated

in the inner barrel of the syringes to reduce the gliding force during administration (Funke et al., 2015; Sacha et al., 2010). However, previous studies have shown an increase in subvisible particles along with an increase in the innate response to its use (Kim et al., 2021; Kim et al., 2022; Krayukhina et al., 2015; Liu et al., 2011; Schargus et al., 2018; Thirumangalathu et al., 2009). Similarly, the current study found a substantial number of subvisible particles in all samples, suggesting a potentially negative impact during and after administration. It has previously been demonstrated that layers of proteins are formed on the silicone oil surface with the primary layer being irreversibly bound whereas subsequent layers are prone to desorption when the plunger is pushed (Couston et al., 2013; Torisu et al., 2017). Consequently, the detached silicone oil and protein films can be swept into the IV bag, causing an increase in the level of microparticles, which was more than 2-fold compared to that of the 60 mg/mL IVIG IV bag prepared by a SO-free syringe (Fig. 2b vs. 6b). Moreover, both the drop shock and agitation further aggravated the particle concentration in Infusion set 1, while agitation induced the highest number of particles (Fig. 6a vs. 6b). Compared to the SO-free syringe, the increment was up to 28-, 3- and 2-fold by agitation in the size ranges 2–10  $\mu\text{m}$ , 10–25  $\mu\text{m}$ , and  $\geq 25 \mu\text{m}$ , respectively, contrary to the 3-, 1.7-, and 3.6-fold increments after the drop shock, respectively. On the other hand, the particle level did not increase in Infusion set 2, indicating the necessity of an in-line filter in the infusion system for protein therapeutics. Surprisingly, the particles  $\geq 25 \mu\text{m}$  were within the limit in either the dropped IVIG IV bag or agitated IVIG samples after infusion, which were from 1 p/mL and 3 p/mL, respectively.

### 3.6. Shape characterization of subvisible particles

One advantage of FI over LO is the characterization of particle morphology based on parameters such as diameter, convexity, circularity, elongation, aspect ratio, etc. Taking advantage of this, characterization of the subvisible particles generated through two infusion sets was performed based on their diameters, circularities, and elongations. The diameter used in this study is derived from the circle with the same area as the projection area of the particle (area-based). Circularity is the ratio of the diameter of a circle with the same size as the projected area and the projected image's perimeter (Promeyrat et al., 2010). Hence, the deviation of shape from a smooth and round circle would reduce the circularity value. Whereas, elongation is the ratio of length/breadth based on the area and perimeter (Camoying and Yñiguez, 2016).

Table 2 depicts the morphological characterization based on diameter, circularity, and elongation, whereas Fig. 7 shows the representative FI images of the subvisible particles generated in IVIG solution after infusion with and without pre-exposure to stresses. Regardless of the stress applied, the mean diameter at all size ranges was greater in Infusion set 1 compared to Infusion set 2 ( $p$ -value:  $< 0.01$ ), signifying the formation of larger sized particles with the use of Infusion set 1 (Table 2). Furthermore, high circularity with low elongation in the size ranges  $\geq 2 \mu\text{m}$  and  $\geq 5 \mu\text{m}$  (since no particles were observed at  $\geq 10 \mu\text{m}$  and  $\geq 25 \mu\text{m}$  in Infusion set 2) were observed in samples infused through Infusion set 2 compared to those of Infusion set 1, indicating the formation of more elongated particles in the later (Fig. 7a, 7d, and 7g vs. Fig. 7b, 7c, 7e, 7f, 7h, and 7i). As the particle size increased, the formation of more fibrous particles was observed, given that circularity decreased, and elongation increased in both infusion sets. Comparable results were obtained in the mechanically stressed samples. However, the elongation was found to be higher in agitated samples in both infusion sets while circularity was reduced in Infusion set 1, suggesting that agitation would generate more elongated fibrous particles compared to the drop stress, also observable through the Fig. 7. This morphological transition of subvisible particles into a more elongated fibrous form resulting from agitation has also been previously documented in IgG1 and IgG4 molecules (Simler et al., 2012). Besides, the agitation has been known to cause aggregation through a variety of processes, including local heat events (Santos et al., 2006) and the facilitation of enhanced contact between the protein and the air-water interface and container surface (Ghazvini et al., 2016). It is possible that

any of these events stimulate structural rearrangement of a specific population of subvisible particles from an amorphous to a more elongated fibrous form (Simler et al., 2012). Similarly, the adsorption and desorption of the layer of proteins during repeated pressing of the tubing in Infusion set 1 might have resulted in particles with lower circularity values ( $p$ -value:  $< 0.001$ ) and higher elongation values ( $p$ -value:  $< 0.001$ ) with a fibrous morphology compared to Infusion set 2. Conversely, the introduction of SO syringes overall increased the circularity even in Infusion set 1, especially at sizes  $\geq 10 \mu\text{m}$  and  $\geq 25 \mu\text{m}$ . This increase in circularity could be attributed mainly to the existence of SO droplets in the samples. Moreover, the FI images in Fig. 7g-7i clearly exhibit the presence of SO droplets characterized by a spherical morphology and a bright inner core.

Additionally, more analysis of morphological characteristics was performed through principal component analysis (PCA) of the datasets presented in Table 2. PCA loadings in Fig. 8a indicate the direction of the plane while PCA score plots exhibited in Fig. 8b indicate the coordinates on the plane. The classification was performed using the positive and negative values of two components (1 and 2). PCA revealed that the two components together explained about 92.5% of the variance in a studied dataset. The first component (PC1) accounted for 80.5% of the variance and was characterized by the strong positive impact of the diameter and elongation parameters on the PC1 component. Similarly, the second component (PC2) accounted for 12% of the variance and was characterized by the positive impact of the circularity and diameter parameters on the PC2 component. Generally, elongation and circularity parameters were considered to affect the shape factor while the diameter parameter was considered to affect the size factor. In this respect, the differently shaped and sized sub-visible particles were projected on the different areas of the score plots with each condition designated with a specific color and symbol (Fig. 8b). The plotted data of condition-agitation appeared to form a distinct ellipse with an inclination towards the positive side of PC1 component, suggesting the significant effect on the shape factor (Fig. 8b, red dotted ellipse). This information verifies Table 2's morphological data, which showed that elongation increased with decreasing circularity and increasing diameter. Whereas the inclusion of the plotted data of condition-SO syringe within an ellipse inclined towards the positive side of PC2 suggested its significant effect on the size factor (Fig. 8b, blue dotted ellipse), which is consistent with the observation as SO increased the circularity at higher size ranges of  $\geq 10 \mu\text{m}$  and  $\geq 25 \mu\text{m}$ . On the other hand, the variance caused solely by

**Table 2**

Morphological characterization of the subvisible particles generated in IVIG solution after passing through Infusion sets 1 and 2 with and without stresses, based on diameter, circularity, and elongation.

Contents		Diameter (SD)				Circularity (SD)				Elongation (SD)			
		$\geq 2 \mu\text{m}^{***}$	$\geq 5 \mu\text{m}^{***}$	$\geq 10 \mu\text{m}^*$	$\geq 25 \mu\text{m}^*$	$\geq 2 \mu\text{m}^{***}$	$\geq 5 \mu\text{m}^{***}$	$\geq 10 \mu\text{m}^{***}$	$\geq 25 \mu\text{m}^*$	$\geq 2 \mu\text{m}^{***}$	$\geq 5 \mu\text{m}^{***}$	$\geq 10 \mu\text{m}^{**}$	$\geq 25 \mu\text{m}^{**}$
Infusion set 1	Without stress	3.97 (0.23)	9.29 (0.73)	16.01 (1.92)	34.07 (4.85)	0.69 (0.08)	0.58 (0.01)	0.48 (0.05)	0.49 (0.17)	3.86 (1.12)	5.87 (0.85)	8.43 (2.06)	9.38 (6.63)
	Bag drop	3.96 (0.36)	8.57 (0.66)	15.60 (2.55)	29.86 (2.89)	0.69 (0.07)	0.57 (0.07)	0.46 (0.07)	0.40 (0.02)	3.42 (0.35)	5.41 (1.44)	8.89 (3.67)	9.52 (4.91)
	Agitation	4.08 (0.15)	8.90 (0.56)	15.96 (1.46)	29.67 (6.48)	0.62 (0.02)	0.47 (0.02)	0.33 (0.04)	0.20 (0.09)	4.62 (0.28)	8.20 (0.73)	14.10 (1.94)	24.58 (5.20)
	SO syringe	4.24 (0.30)	9.03 (0.69)	15.72 (1.29)	31.74 (8.19)	0.85 (0.02)	0.79 (0.02)	0.73 (0.04)	0.41 (0.09)	1.92 (0.28)	2.39 (0.73)	2.87 (1.94)	8.96 (5.20)
Infusion set 2	Without stress	2.79 (0.53)	5.85 (0.78)	NA	NA	0.84 (0.08)	0.73 (0.34)	NA	NA	1.78 (0.92)	3.19 (3.09)	NA	NA
	Bag drop	3.08 (0.36)	8.33 (1.48)	14.81 (2.05)	NA	0.87 (0.09)	0.68 (0.30)	0.76 (0.02)	NA	2.12 (1.34)	1.54 (0.06)	2.06 (0.25)	NA
	Agitation	3.14 (0.20)	8.07 (1.48)	13.86 (3.85)	26.69 (1.75)	0.92 (0.01)	0.84 (0.03)	0.64 (0.03)	0.64 (0.15)	1.32 (0.06)	2.24 (0.74)	7.36 (6.19)	20.11 (1.37)
	SO syringe	3.36 (0.41)	7.78 (3.12)	15.07 (3.70)	29.79 (2.93)	0.86 (0.04)	0.72 (0.10)	0.53 (0.02)	0.58 (0.22)	2.39 (1.51)	3.16 (0.99)	6.25 (1.04)	3.46 (2.46)

\* $p < 0.05$ , \*\* $p < 0.01$ , and \*\*\* $p < 0.001$ , indicates statistically significant difference between the set of data in Infusion set 1 and Infusion set 2 based on diameter, circularity, and elongation at different size ranges.

SD: standard deviation.

NA: data not available.

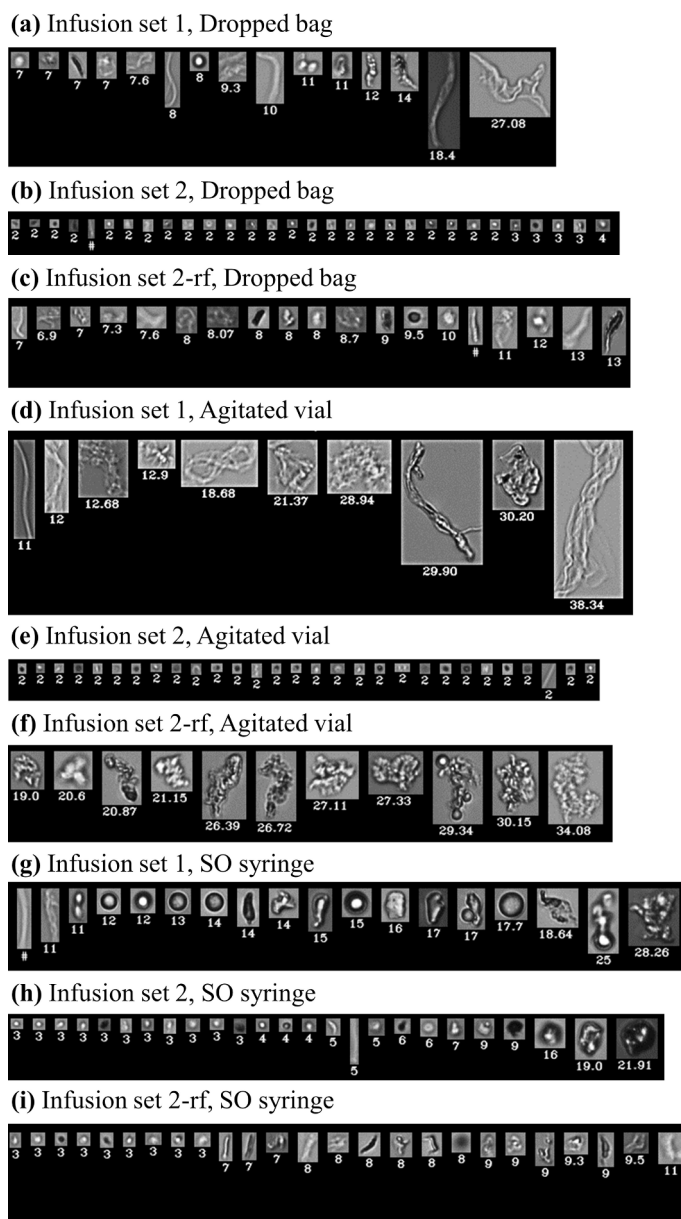


**Fig. 7.** Representative FI images of subvisible particles generated after infusion of samples pre-exposed to the drop shock (a-c), agitation (d-f), and SO syringes (g-i).

condition-bag drop or condition-without stress was within a 95% confidence ellipse (Fig. 8b, solid black lined ellipse), indicating less effect in the particle characterization. Overall, the data illustrates that in addition to the size, the particle morphological character can also be utilized to define the protein subvisible particle population based on different stresses. As subvisible particles are a persistent issue in biopharmaceuticals, identifying them is crucial for determining their source and thus optimizing the formulation development or avoiding them in the manufacturing process. Moreover, the FI technique allows for a quantitative study of these morphological features, allowing for a more precise understanding of protein aggregation.

### 3.7. Limitation of gravity-based infusion

During the preliminary study, the experiment was designed with three different IVIG concentrations; 20 mg/mL, 60 mg/mL, and 100 mg/mL. At 100 mg/mL, it was directly connected to the infusion set through the bottle (Fig. 9). The infusion was conducted smoothly with Infusion set 1, whereas flow resistance was observed at 100 mg/mL IVIG with

Infusion set 2. In other words, the in-line flow was stopped. As a further investigation, the viscosity of IVIG was measured within a range of concentration from 60 mg/mL to 100 mg/mL with an increasing shear rate. The viscosity of IVIG was consequently reduced with increasing shear stress exhibiting a non-Newtonian-like behavior (Fig. 9). The initial viscosity of 2.46 mPa·s at 2100 s<sup>-1</sup> decreased to 2.28 at a shear rate 9900 s<sup>-1</sup> at 60 mg/mL IVIG. Moreover, the viscosity increased as the IVIG concentration increased since viscosities in concentrated solutions are induced by both molecular crowding as the fraction of solvent declines and by direct interactions between protein molecules (Galush et al., 2012). Furthermore, the same samples were allowed to run through both IV infusion sets. As observed at the beginning of the experiment, all the samples freely passed through Infusion set 1, whereas only up to 70 mg/mL could pass through Infusion set 2. Once the filter was removed from Infusion set 2, the permittance changed to 80 mg/mL. Since a negative pressure is created in Infusion set 1 with the peristaltic motion, easy forward movement of all the concentrations was observed. However, Infusion set 2 is particularly based on the gravitational forces, resulting in the flow resistance in the samples higher than

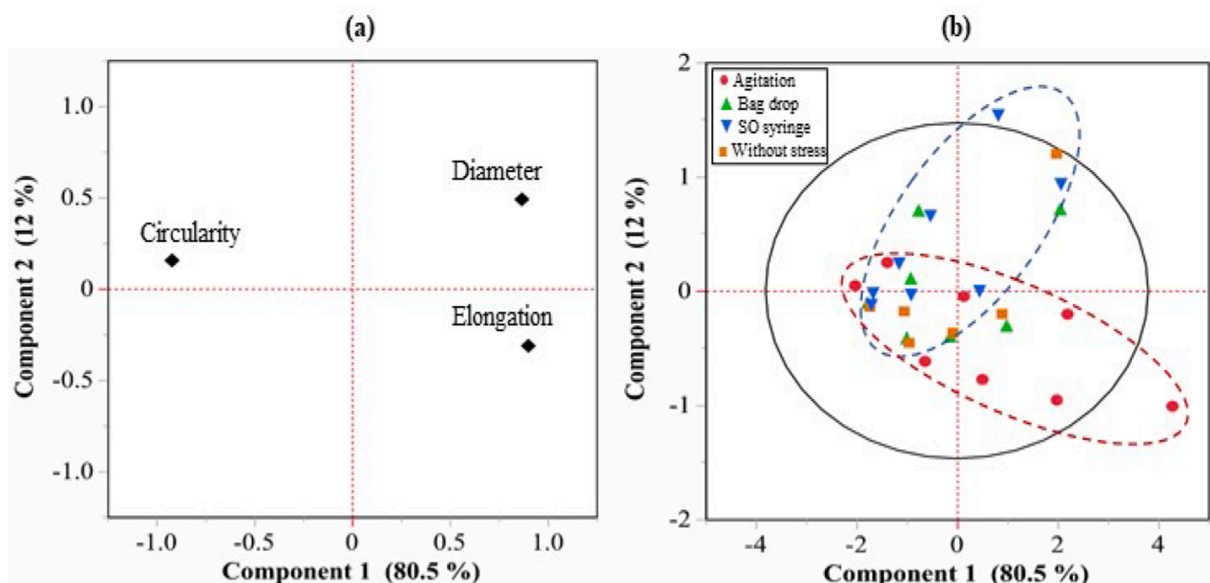


Fig. 8. (a) PCA loadings of the parameters and (b) PCA score plots of the sub-visible particles under different conditions: agitation (red circle), bag drop (green triangle), SO syringe (blue inverted triangle), and without stress (orange square). (For interpretation of the references to color in this figure legend, the reader is referred to the web version of this article.)

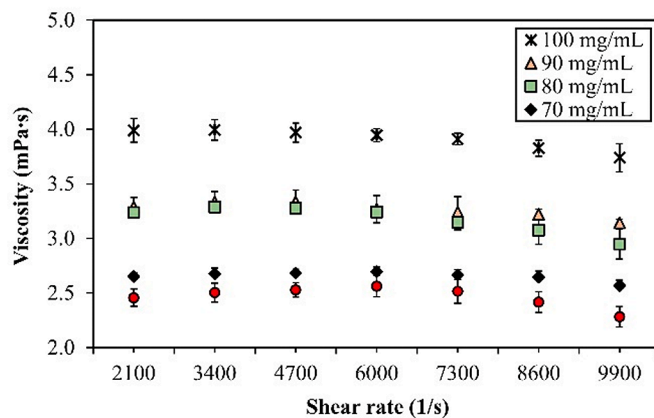
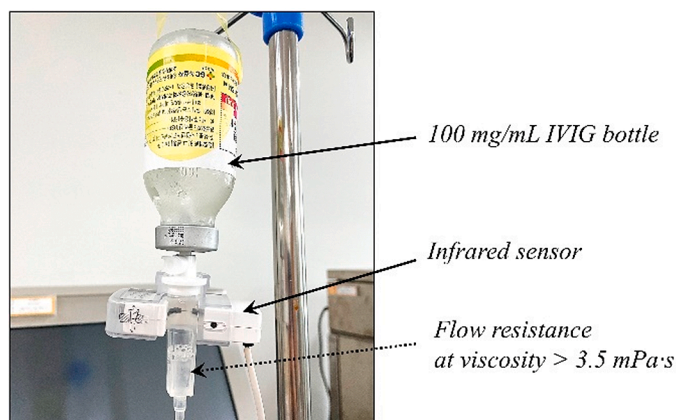


Fig. 9. Graph plot of viscosity vs. shear of IVIG solutions in the concentrations ranging from 60 mg/mL to 100 mg/mL (on the right) and a photographic image showing the flow resistance in 100 mg/mL IVIG solution through Infusion set 1 (on the left).

the viscosity of around 3 mPa·s. Hence, although gravity infusion sets with filters have shown remarkable results in preventing the generation of particulate matter, one limitation of this set might be the limit in the infusion of protein formulations with high viscosities.

### 3.8. Future perspectives

Compounding pharmacists and healthcare providers are expected to administer safe and effective pharmaceutical dosages within a certain period. Given the length of time between preparation and administration, healthcare providers also have the responsibility to ensure the intactness of the stability of the product in its final administrated form. However, the guidelines or instructions related to the preparation or administration process seem to lack warnings regarding this. The current study reveals that even careful preparation of IV infusions, without any mishandling such as shaking or dropping, can lead to the generation of subvisible particles that could exceed the limit specified in USP chapter <787> depending on the infusion set and tubing. **Accu-Drip**, a gravity-based precision infusion system, prevents the formation of particulate matter by limiting the mechanical stress on the infusion tube.

Moreover, the presence of a 5- $\mu$ m in-line filter reduces the passage of particles  $\geq 10 \mu$ m, showing the importance of filters in the tubing line. However, no indication exists regarding its use as in the case of IVIG where a huge range of filter sizes has been recommended starting from 0.2- $\mu$ m to 200- $\mu$ m filters (Werner and Winter, 2015). A study done in 2015 with more than 300 marketed therapeutic proteins revealed that only 16 % of the products were filtered (44.6% during preparation and 55.4% during administration) with a large number of products without any filtration recommendation, along with which a broad variation in filter pore size recommendation was also found (Werner and Winter, 2015). Nevertheless, the remarkable difference between the peristaltic pump and gravity infusion systems along with the silicone oil-lubricated and silicone oil-free syringes on the level of subvisible particles, suggests a proper selection of the administration devices for the safety of the patients and to maintain the efficacy of the treatment.

### 4. Conclusion

The presence of subvisible particles in medicinal preparations is considered a major challenge in developing biopharmaceuticals. This is

especially problematic during IV infusion since the patients are exposed to a high volume of the drug product over an extended period. With the growing need for IV infusion systems having precise flow rates and pressure, infusion pumps with high relative accuracy have grown in popularity. However, this study found that infusion pumps with peristaltic systems are more susceptible to particle production due to the constant pressure into the tube. When the infusion set with a gravity system was applied, however, a significant drop in the subvisible particle concentration was found. Furthermore, the presence of an in-line filter in the tubing system of the gravity infusion set prevented particles from passing through the infusion line. Moreover, the manufacturer claims that the **Accu-drip** infusion set used in this experiment has an accuracy of 3% owing to the presence of a drip sensor attached to an automated infusion control mechanism. The restriction would be the flow resistance that may arise in high-viscosity medicinal preparations. Based on the results, this study suggests appropriate infusion sets based on compatibility tests and the need for an IV-line set equipped with an in-line filter. Furthermore, the study raises awareness of the few mishandlings that often occur in the clinical setting, as well as the consequences of using off-label use syringes, prompting the proper indication and guidelines in handling biotherapeutics.

#### CRedit authorship contribution statement

**Shavron Hada:** Data curation, Methodology, Writing – original draft. **Sunkyong Ji:** Data curation, Methodology. **Ye Na Lee:** Methodology. **Ki Hyun Kim:** Conceptualization, Writing – review & editing. **Ravi Maharjan:** Methodology. **Nam Ah Kim:** Conceptualization, Methodology, Writing – review & editing. **Jukka Rantanen:** Conceptualization. **Seong Hoon Jeong:** Conceptualization, Methodology, Writing – review & editing.

#### Declaration of Competing Interest

The authors declare that they have no known competing financial interests or personal relationships that could have appeared to influence the work reported in this paper.

#### Data availability

Data will be made available on request.

#### Acknowledgment

This study was supported by the National Research Foundation of Korea grant funded by the Korean government (NRF-2018R1A5A2023127 and NRF-2019R1A2C1083911). Special thanks to **Hanvit MD** for designing the accurate gravity-based infusion system with technical support from the Korea Aerospace Research Institute.

#### References

- Al Salloum, H., Saunier, J., Dazzi, A., Vigneron, J., Etcheberry, A., Marlière, C., Aymes-Chodur, C., Herry, J.M., Bernard, M., Jubeli, E., Yagoubi, N., 2017. Characterization of the surface physico-chemistry of plasticized PVC used in blood bag and infusion tubing. *Mater. Sci. Eng.* 75, 317–334.
- Allcutt, D., Lort, D., McCollum, C., 1983. Final inline filtration for intravenous infusions: a prospective hospital study. *Br. J. Surg.* 70, 111–113. <https://doi.org/10.1002/bjs.1800700219>.
- Bernard, L., Cuff, R., Breyse, C., Décaudin, B., Sautou, V., 2015. Migrability of PVC plasticizers from medical devices into a simulant of infused solutions. *Int. J. Pharm.* 485 (1–2), 341–347.
- Besheer, A., 2017. Protein adsorption to in-line filters of intravenous administration sets. *J. Pharm. Sci.* 106, 2959–2965. <https://doi.org/10.1016/j.xphs.2017.05.028>.
- Camoying, M.G., Yñiguez, A.T., 2016. FlowCAM optimization: attaining good quality images for higher taxonomic classification resolution of natural phytoplankton samples. *Limnol. Oceanogr.: Methods* 14, 305–314. <https://doi.org/10.1002/lom3.10090>.
- Carpenter, J.F., Randolph, T.W., Jiskoot, W., Crommelin, D.J.A., Russell Middaugh, C., Winter, G., Fan, Y.-X., Kirshner, S., Verthelyi, D., Kozlowski, S., Clouse, K.A.,

- Swann, P.G., Rosenberg, A., Cherney, B., 2009. Overlooking subvisible particles in therapeutic protein products: gaps that may compromise product quality. *J. Pharm. Sci.* 98 (4), 1201–1205.
- Council, E., 2007. Directive 2007/47/EC of the European Parliament and of the Council of 5 September 2007. *Official J. Eur. Union*.
- Couston, R.G., Skoda, M.W., Uddin, S., van der Walle, C.F., 2013. Adsorption behavior of a human monoclonal antibody at hydrophilic and hydrophobic surfaces. *mAbs* 5 (1), 126–139.
- Crass, R.E., Vance, J.R., 1985. In vivo accuracy of gravity-flow iv infusion systems. *Am. J. Hosp. Pharm.* 42, 328–331. <https://doi.org/10.1093/ajhp/42.2.328>.
- Cromwell, M.E., Hilario, E., Jacobson, F., 2006. Protein aggregation and bioprocessing. *AAPS J.* 8, E572–E579. <https://doi.org/10.1208/aapsj080366>.
- Deiringer, N., Friess, W., 2022a. Proteins on the Rack: mechanistic studies on protein particle formation during peristaltic pumping. *J. Pharm. Sci.* 111, 1370–1378. <https://doi.org/10.1016/j.xphs.2022.01.035>.
- Deiringer, N., Friess, W., 2022b. Reaching the breaking point: effect of tubing characteristics on protein particle formation during peristaltic pumping. *Int. J. Pharm.* 627, 122216. <https://doi.org/10.1016/j.ijpharm.2022.122216>.
- Deiringer, N., Friess, W., 2023. Afraid of the wall of death? Considerations on monoclonal antibody characteristics that trigger aggregation during peristaltic pumping. *Int. J. Pharm.* 633, 122635. <https://doi.org/10.1016/j.ijpharm.2023.122635>.
- Deiringer, N., Rüdiger, D., Luxbacher, T., Zahler, S., Frieß, W., 2022. Catching speedy gonzales: driving forces for protein film formation on silicone rubber tubing during pumping. *J. Pharm. Sci.* 111, 1577–1586. <https://doi.org/10.1016/j.xphs.2022.02.013>.
- Dreckmann, T., Boeuf, J., Ludwig, I.-S., Lümekemann, J., Huwlyer, J., 2020. Low volume aseptic filling: impact of pump systems on shear stress. *Eur. J. Pharm. Biopharm.* 147, 10–18. <https://doi.org/10.1016/j.ejpb.2019.12.006>.
- Earla, A., Braslau, R., 2014. Covalently Linked Plasticizers: Triazole Analogues of Phthalate Plasticizers Prepared by Mild Copper-Free “Click” Reactions with Azide-Functionalized PVC. *Macromol. Rapid Commun.* 35, 666–671. <https://doi.org/10.1002/marc.201300865>.
- Fawaz, I., Schaz, S., Boehrer, A., Garidel, P., Blech, M., 2023. Micro-Flow Imaging multi-instrument evaluation for sub-visible particle detection. *Eur. J. Pharm. Biopharm.* 185, 55–70.
- Formato, G., Romano, R., Formato, A., Sorvari, J., Koiranen, T., Pellegrino, A., Villecco, F., 2019. Fluid-structure interaction modeling applied to peristaltic pump flow simulations. *Machines* 7, 50. <https://doi.org/10.3390/machines7030050>.
- Funke, S., Matilainen, J., Nalenz, H., Bechtold-Peters, K., Mahler, H.-C., Friess, W., 2015. Analysis of thin baked-on silicone layers by FTIR and 3D-Laser Scanning Microscopy. *Eur. J. Pharm. Biopharm.* 96, 304–313. <https://doi.org/10.1016/j.ejpb.2015.08.009>.
- Galush, W.J., Le, L.N., Moore, J.M., 2012. Viscosity behavior of high-concentration protein mixtures. *J. Pharm. Sci.* 101, 1012–1020. <https://doi.org/10.1002/jps.23002>.
- Ghazvini, S., Kalonia, C., Volkin, D.B., Dhar, P., 2016. Evaluating the role of the air-solution interface on the mechanism of subvisible particle formation caused by mechanical agitation for an IgG1 mAb. *J. Pharm. Sci.* 105, 1643–1656. <https://doi.org/10.1016/j.xphs.2016.02.027>.
- Glover, Z.W.K., Gennaro, L., Yadav, S., Demeule, B., Wong, P.Y., Sreedhara, A., 2013. Compatibility and stability of pertuzumab and trastuzumab admixtures in i.v. infusion bags for coadministration. *J. Pharm. Sci.* 102, 794–812. <https://doi.org/10.1002/jps.23403>.
- Gomme, P.T., Hunt, B.M., Tatford, O.C., Johnston, A., Bertolini, J., 2006. Effect of lobe pumping on human albumin: investigating the underlying mechanisms of aggregate formation 1. *Biotechnol. Appl. Biochem.* 43, 103–111. <https://doi.org/10.1042/BA20050147>.
- Helbig, C., Ammann, G., Menzen, T., Friess, W., Wuchner, K., Hawe, A., 2020. Backgrounded membrane imaging (BMI) for high-throughput characterization of subvisible particles during biopharmaceutical drug product development. *J. Pharm. Sci.* 109, 264–276. <https://doi.org/10.1016/j.xphs.2019.03.024>.
- Her, C., Carpenter, J.F., 2020. Effects of tubing type, formulation, and postpumping agitation on nanoparticle and microparticle formation in intravenous immunoglobulin solutions processed with a peristaltic filling pump. *J. Pharm. Sci.* 109, 739–749. <https://doi.org/10.1016/j.xphs.2019.05.013>.
- Her, C., Tanenbaum, L.M., Bandi, S., Randolph, T.W., Thirumangalathu, R., Mallela, K.M., Carpenter, J.F., Elias, Y., 2020. Effects of tubing type, operating parameters, and surfactants on particle formation during peristaltic filling pump processing of a mAb formulation. *J. Pharm. Sci.* 109, 1439–1448. <https://doi.org/10.1016/j.xphs.2020.01.009>.
- Hung, J.C., 2004. Commentary: USP general chapter < 797 > pharmaceutical compounding-sterile preparations. *J. Nucl. Med.* 45, 20N–N. <https://jnm.snmjournals.org/content/jnumed/45/6/20N.full.pdf>.
- Illum, L., Davis, S., Wilson, C., Thomas, N., Frier, M., Hardy, J., 1982. Blood clearance and organ deposition of intravenously administered colloidal particles. the effects of particle size, nature and shape. *Int. J. Pharm.* 12, 135–146. [https://doi.org/10.1016/0378-5173\(82\)90113-2](https://doi.org/10.1016/0378-5173(82)90113-2).
- Jiskoot, W., Nejadnik, M.R., Sediq, A.S., 2017. Potential issues with the handling of biologicals in a hospital. *J. Pharm. Sci.* 106, 1688–1689. <https://doi.org/10.1016/j.xphs.2017.02.029>.
- Kamerzell, T.J., Esfandiari, R., Joshi, S.B., Middaugh, C.R., Volkin, D.B., 2011. Protein–excipient interactions: mechanisms and biophysical characterization applied to protein formulation development. *Adv. Drug Delivery Rev.* 63, 1118–1159. <https://doi.org/10.1016/j.addr.2011.07.006>.

- Khan, T.A., Mahler, H.-C., Kishore, R.S., 2015. Key interactions of surfactants in therapeutic protein formulations: a review. *Eur. J. Pharm. Biopharm.* 97, 60–67. <https://doi.org/10.1016/j.ejpb.2015.09.016>.
- Kim, N.A., Kim, D.J., Jeong, S.H., 2020. Do not flick or drop off-label use plastic syringes in handling therapeutic proteins before administration. *Int. J. Pharm.* 587, 119704. <https://doi.org/10.1016/j.ijpharm.2020.119704>.
- Kim, N.A., Hada, S., Kim, D.J., Choi, D.H., Jeong, S.H., 2021. Off-label use of plastic syringes with silicone oil for intravenous infusion bags of antibodies. *Eur. J. Pharm. Biopharm.* 166, 205–215. <https://doi.org/10.1016/j.ejpb.2021.07.001>.
- Kim, H.L., Mcauley, A., Livesay, B., Gray, W.D., McGuire, J., 2014. Modulation of protein adsorption by poloxamer 188 in relation to polysorbates 80 and 20 at solid surfaces. *J. Pharm. Sci.* 103, 1043–1049. <https://doi.org/10.1002/jps.23907>.
- Kim, N.A., Noh, G.Y., Hada, S., Na, K.J., Yoon, H.-J., Park, K.-W., Park, Y.-M., Jeong, S. H., 2022. Enhanced protein aggregation suppressor activity of N-acetyl-L-arginine for agitation-induced aggregation with silicone oil and its impact on innate immune responses. *Int. J. Biol. Macromol.* 216, 42–51. <https://doi.org/10.1016/j.ijbiomac.2022.06.176>.
- Klespitz, J., Kovács, L., 2014. Peristaltic pumps—A review on working and control possibilities, 2014 IEEE 12th International Symposium on Applied Machine Intelligence and Informatics (SAM). *IEEE*, pp. 191–194. 10.1109/SAMI.2014.6822404.
- Krayukhina, E., Tsumoto, K., Uchiyama, S., Fukui, K., 2015. Effects of syringe material and silicone oil lubrication on the stability of pharmaceutical proteins. *J. Pharm. Sci.* 104, 527–535. <https://doi.org/10.1002/jps.24184>.
- Kumru, O.S., Liu, J., Ji, J.A., Cheng, W., Wang, Y.J., Wang, T., Joshi, S.B., Middaugh, C. R., Volkin, D.B., 2012. Compatibility, physical stability, and characterization of an IgG4 monoclonal antibody after dilution into different intravenous administration bags. *J. Pharm. Sci.* 101, 3636–3650. <https://doi.org/10.1002/jps.23224>.
- Langille, S.E., 2013. Particulate matter in injectable drug products. *PDA J. Pharm. Sci. Technol.* 67, 186–200. <https://doi.org/10.5731/pdajpst.2013.00922>.
- Linkuvienė, V., Ross, E.L., Crawford, L., Weiser, S.E., Man, D., Kay, S., Kolhe, P., Carpenter, J.F., 2022. Effects of transportation of IV bags containing protein formulations via hospital pneumatic tube system: particle characterization by multiple methods. *J. Pharm. Sci.* 111, 1024–1039. <https://doi.org/10.1016/j.xphs.2022.01.016>.
- Liu, L., Ammar, D.A., Ross, L.A., Mandava, N., Kahook, M.Y., Carpenter, J.F., 2011. Silicone oil microdroplets and protein aggregates in repackaged bevacizumab and ranibizumab: effects of long-term storage and product mishandling. *Invest. Ophthalmol. Visual Sci.* 52, 1023–1034. <https://doi.org/10.1167/iov.10-6431>.
- Luo, S., McSweeney, K.M., Wang, T., Bacot, S.M., Feldman, G.M., Zhang, B., 2020. Defining the right diluent for intravenous infusion of therapeutic antibodies, *mAbs*. Taylor & Francis, p. 1685814.
- Maa, Y.F., Hsu, C.C., 1996. Effect of high shear on proteins. *Biotechnol. Bioeng.* 51, 458–465. [https://doi.org/10.1002/\(SICI\)1097-0290\(19960820\)51:4%3C458::AID-BIT9%3E3.0.CO;2-H](https://doi.org/10.1002/(SICI)1097-0290(19960820)51:4%3C458::AID-BIT9%3E3.0.CO;2-H).
- Marx, A., 2019. An investigation of the long term chemical stability and physical performance of PMD-citronellal acetal compared with dibutyl phthalate and BIS (2-ethylhexyl) terephthalate as plasticisers in selected cosmetic formulations. Nelson Mandela University Theses and Dissertations. [http://vital.seals.ac.za:8080/vital/access/manager/Repository/vital:36669?site\\_name=GlobalView](http://vital.seals.ac.za:8080/vital/access/manager/Repository/vital:36669?site_name=GlobalView).
- Matos, M., Cordeiro, R.A., Faneca, H., Coelho, J.F., Silvestre, A.J., Sousa, A.F., 2019. Replacing Di(2-ethylhexyl) Terephthalate by Di(2-ethylhexyl) 2,5-Furandicarboxylate for PVC plasticization: synthesis, Mater. Preparation and Characterization. *Mater.* 12, 2336. <https://doi.org/10.3390/ma12142336>.
- McLeod, A., Walker, I., Zheng, S., Hayward, C., 2000. Loss of factor VIII activity during storage in PVC containers due to adsorption. *Haemophilia: the Official J. World Federation of Hemophilia* 6, 89–92. <https://doi.org/10.1046/j.1365-2516.2000.00382.x>.
- Messina, K.M.M., Woys, A.M., 2023. Random heteropolymer excipients improve the colloidal stability of a monoclonal antibody for subcutaneous administration. *Pharm. Res.* 40 (2), 525–536.
- Nejadnik, M.R., Randolph, T.W., Volkin, D.B., Schöneich, C., Carpenter, J.F., Crommelin, D.J., Jiskoot, W., 2018. Postproduction handling and administration of protein pharmaceuticals and potential instability issues. *J. Pharm. Sci.* 107, 2013–2019. <https://doi.org/10.1016/j.xphs.2018.04.005>.
- Niehaus, G., Saba, T., Edmonds, R., Dillon, B., 1984. Leukocyte involvement in pulmonary localization of blood-borne microparticulates: relationship to altered lung fluid balance. *Circ. Shock* 12, 95–105. <https://europepmc.org/article/med/6705154>.
- Panchal, J., Falk, B.T., Antochshuk, V., McCoy, M.A., 2022. Investigating protein–excipient interactions of a multivalent VHH therapeutic protein using NMR spectroscopy, *mAbs*. Taylor & Francis, p. 2124902.
- Pardeshi, N.N., Qi, W., Dahl, K., Caplan, L., Carpenter, J.F., 2017. Microparticles and nanoparticles delivered in intravenous saline and in an intravenous solution of a therapeutic antibody product. *J. Pharm. Sci.* 106, 511–520. <https://doi.org/10.1016/j.xphs.2016.09.028>.
- Pardeshi, N.N., Ahmadi, M., Sierzputowska, I., Fogg, M., Baker, M., Carpenter, J.F., 2021. Subvisible particles in solutions of remicade in intravenous saline activate immune system pathways in in vitro human cell systems. *J. Pharm. Sci.* 110, 2894–2903. <https://doi.org/10.1016/j.xphs.2021.04.005>.
- Pollo, M., Mehta, A., Torres, K., Thorne, D., Zimmermann, D., Kolhe, P., 2019. Contribution of intravenous administration components to subvisible and submicron particles present in administered drug product. *J. Pharm. Sci.* 108, 2406–2414. <https://doi.org/10.1016/j.xphs.2019.02.020>.
- Promeyrat, A., Bax, M.-L., Traore, S., Aubry, L., Sante-Lhoutellier, V., Gatellier, P., 2010. Changed dynamics in myofibrillar protein aggregation as a consequence of heating time and temperature. *Meat Sci.* 85, 625–631. <https://doi.org/10.1016/j.meatsci.2010.03.015>.
- Randolph, T.W., Schiltz, E., Sederstrom, D., Steinmann, D., Mozziconacci, O., Schöneich, C., Freund, E., Ricci, M.S., Carpenter, J.F., Lengsfeld, C.S., 2015. Do not drop: mechanical shock in vials causes cavitation, protein aggregation, and particle formation. *J. Pharm. Sci.* 104, 602–611. <https://doi.org/10.1002/jps.24259>.
- Rock, G., Labow, R.S., Tocchi, M., 1986. Distribution of di (2-ethylhexyl) phthalate and products in blood and blood components. *Environ. Health Perspect.* 65, 309–316. <https://doi.org/10.1289/ehp.8665309>.
- Sacha, G.A., Saffell-Clemmer, W., Abram, K., Akers, M.J., 2010. Practical fundamentals of glass, rubber, and plastic sterile packaging systems. *Pharm. Dev. Technol.* 15, 6–34. <https://doi.org/10.3109/10837450903511178>.
- Santos, O., Nylander, T., Paulsson, M., Trägårdh, C., 2006. Whey protein adsorption onto steel surfaces—effect of temperature, flow rate, residence time and aggregation. *J. Food Eng.* 74, 468–483. <https://doi.org/10.1016/j.jfoodeng.2005.03.037>.
- Schargin, M., Werner, B.P., Geerling, G., Winter, G., 2018. Contamination of anti-VEGF drugs for intravitreal injection: how do repackaging and newly developed syringes affect the amount of silicone oil droplets and protein aggregates? *Retina* 38, 2088–2095. <https://doi.org/10.1097/IAE.0000000000001809>.
- Sherwin, C.M., Medicott, N.J., Reith, D.M., Broadbent, R.S., 2014. Intravenous drug delivery in neonates: lessons learnt. *Arch. Dis. Child.* 99, 590–594. <https://doi.org/10.1136/archdischild-2013-304887>.
- Simler, B.R., Hui, G., Dahl, J.E., Perez-Ramirez, B., 2012. Mechanistic complexity of subvisible particle formation: links to protein aggregation are highly specific. *J. Pharm. Sci.* 101, 4140–4154. <https://doi.org/10.1002/jps.23299>.
- Snell, J.R., Monticello, C.R., Her, C., Ross, E.L., Frazer-Abel, A.A., Carpenter, J.F., Randolph, T.W., 2020. DEHP nanodroplets leached from polyvinyl chloride IV bags promote aggregation of IVIG and activate complement in human serum. *J. Pharm. Sci.* 109, 429–442. <https://doi.org/10.1016/j.xphs.2019.06.015>.
- Sreedhara, A., Glover, Z.K., Piro, N., Xiao, N., Patel, A., Kabakoff, B., 2012. Stability of IgG1 Monoclonal Antibodies in Intravenous Infusion Bags Under Clinical In-Use Conditions. *J. Pharm. Sci.* 101, 21–30. <https://doi.org/10.1002/jps.22739>.
- Svilenov, H.L., Kopp, K.T., Golovanov, A.P., Winter, G., Zalar, M., 2023. Insights into the stabilization of interferon alpha by two surfactants revealed by STD-NMR spectroscopy. *J. Pharm. Sci.* 112, 404–410. <https://doi.org/10.1016/j.xphs.2022.10.013>.
- Szycher, M., Comparative Chemical Resistance of Polyurethanes. A Critical Review. <http://www.flomedicalsales.com.au/wp-content/uploads/White-paper-Carbothane.pdf>.
- Thirumangalathu, R., Krishnan, S., Ricci, M.S., Brems, D.N., Randolph, T.W., Carpenter, J.F., 2009. Silicone oil- and agitation-induced aggregation of a monoclonal antibody in aqueous solution. *J. Pharm. Sci.* 98, 3167–3181. <https://doi.org/10.1002/jps.21719>.
- Thomas, C., Geer, D., 2011. Effects of shear on proteins in solution. *Biotechnol. Lett.* 33, 443–456. <https://doi.org/10.1007/s10259-010-0469-4>.
- Torisu, T., Maruno, T., Yoneda, S., Hamaji, Y., Honda, S., Ohkubo, T., Uchiyama, S., 2017. Friability testing as a new stress-stability assay for biopharmaceuticals. *J. Pharm. Sci.* 106, 2966–2978. <https://doi.org/10.1016/j.xphs.2017.05.035>.
- Turco, S.J., Davis, N.M., 1971. Detrimental effects of particulate matter on the pulmonary circulation. *JAMA* 217, 81–82. <https://doi.org/10.1001/jama.1971.03190010063029>.
- Tzannis, S.T., Hrushesky, W.J., Wood, P.A., Przybycien, T.M., 1997. Adsorption of a formulated protein on a drug delivery device surface. *J. Colloid Interface Sci.* 189, 216–228. <https://doi.org/10.1006/jcis.1997.4841>.
- Ueda, T., Nakamura, K., Abe, Y., Carpenter, J.F., 2019. Effects of product handling parameters on particle levels in a commercial factor VIII product: impacts and mitigation. *J. Pharm. Sci.* 108, 775–786. <https://doi.org/10.1016/j.xphs.2018.08.022>.
- Van Boxel, T., Pittiruti, M., Arkema, A., Ball, P., Barone, G., Bertoglio, S., Biffi, R., Dupont, C., Fonzo-Christe, C., Foster, J., Jones, M., Keck, C., Ray-Barruel, G., Sasse, M., Scoppettuolo, G., Van Den Hoogen, A., Villa, G., Hadaway, L., Ryder, M., Schears, G., Stone, J., 2022. WoCoVA consensus on the clinical use of in-line filtration during intravenous infusions: current evidence and recommendations for future research. *J. Vasc. Access* 23 (2), 179–191.
- Werner, B.P., Winter, G., 2015. Particle contamination of parenteral and in-line filtration of proteinaceous drugs. *Int. J. Pharm.* 496, 250–267. <https://doi.org/10.1016/j.ijpharm.2015.10.082>.
- Wu, H., Randolph, T.W., 2020. Aggregation and particle formation during pumping of an antibody formulation are controlled by electrostatic interactions between pump surfaces and protein molecules. *J. Pharm. Sci.* 109, 1473–1482. <https://doi.org/10.1016/j.xphs.2020.01.023>.
- Yoneda, S., Niederleitner, B., Wiggernhorn, M., Koga, H., Totoki, S., Krayukhina, E., Friess, W., Uchiyama, S., 2019. Quantitative laser diffraction for quantification of protein aggregates: comparison with resonant mass measurement, nanoparticle tracking analysis, flow imaging, and light obscuration. *J. Pharm. Sci.* 108, 755–762. <https://doi.org/10.1016/j.xphs.2018.09.004>.
- Zahid, N., Taylor, K.M., Gill, H., Maguire, F., Schulman, R., 2008. Adsorption of insulin onto infusion sets used in adult intensive care unit and neonatal care settings. *Diabetes Res. Clin. Pract.* 80, e11–e13. <https://doi.org/10.1016/j.diabres.2008.02.013>.